Neural Network for Reconstruction of MPI Images

P. Koch[a*], M. Maass[a], M. Bruhns[a], C. Droigk[a], T. J. Parbs[a], and A. Mertins[a]

[a] *Institute for Signal Processing, University of Lübeck, Germany*
[*] *Corresponding author, email: koch@isip.uni-luebeck.de*

Abstract: In Magnetic Particle Imaging the reconstruction of the image given the voltage signal is not trivial. Since the system function cannot be measured in its entirety the reconstruction algorithms can only estimate the images. The standard reconstruction approaches usually rely on time consuming optimization concepts that involve the use of sophisticated priors. We studied the general possibility of learning the reconstruction with neural networks. The results reveal that the networks potentially can reconstruct the images while even learning priors. However, the structures used for harvesting the training data should be chosen wisely.

I. Introduction

In Magnetic Particle Imaging (MPI), voltage signals induced by superparamagnetic nanoparticles are acquired from which the particle distributions have to be reconstructed. One approach for reconstruction is based on the system matrix. Given the estimated system matrix, one common way to deal with the reconstruction is based on iterative algorithms like the Kaczmarz method [1]. Thus, the reconstruction of an image is usually an iterative optimization process that is often time consuming. The same holds when sophisticated priors are used for regularization. An alternative is to learn the inverse system in a data-driven fashion. For this purpose, machine learning techniques from the field of neural networks (NNs) can be adopted. First attempts to use neural networks for the particle distribution reconstruction have already been made [2,3]. However, both of these methods work in the frequency space, with only one-dimensional trajectory for the drive fields. Also, only dense NNs were used. In contrast, the method proposed here works with two-dimensional trajectory and operates in the time domain. Arguably, it appears promising to adopt so-called convolutional neural networks (CNNs). For example, in [4] CNNs were used for denoising and reconstruction of computed tomography images. Furthermore, CNNs have been adopted to reconstruct images of general inverse problems [5,6]. Due to the success of CNNs, we use this type of network for reconstruction of MPI images.

II. Material and Methods

II.I. Convolutional Neural Network

In this work, we propose a fairly small architecture (see Fig. 1). The network is similar to the one in [7] used for reconstruction of e.g. magnetic tomography images. The input of the network is the measured voltage signal as a vector. The first two layers of the network are dense layers. The size of the second dense layer defines the size of the reconstructed image. Subsequently, 2D convolution layers are deployed. The multiple feature maps produced by the first convolution

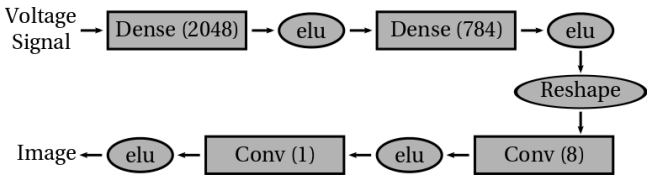

Figure 1: *Network architecture. Dense indicates a dense layer, where its size is specified in parenthesis. Conv denotes a 2D-convolution layer, where the number of 3x3 kernels is given in parenthesis. The reshape block represents the transition from a 1D signal to a 2D image (28x28 pixels).*

layer are fused to a single image by the single kernel of the second convolution layer. Thus, the output of the network is the reconstructed image. As activation function we used the exponential linear unit (elu)

$$f(\alpha, x) = \begin{cases} \alpha(e^x - 1), \text{ for } x < 0 \\ x, \text{ for } x \geq 0 \end{cases} \qquad (1)$$

with $\alpha = 0.1$ for our experiments. This feed-forward network is trained in a supervised fashion. We tried two different loss functions: mean squared error (MSE) and mean absolute error (MAE) between the network's output and the ground truth. The loss is used to adapt the weights using the Adam optimizer.

II.II Test Setup

As a reference system, a linear minimum MSE (MMSE) estimator followed by a non-negativity constraint was used [8]. Given the observed signal u, an estimate $\hat{c}$ for the particle distribution c is calculated by $\hat{c} = \max(A \cdot (u - \bar{u}) + \bar{c},\ 0)$, where

$$A = E\{(c - \bar{c})(u - \bar{u})^T\} E\{(u - \bar{u})(u - \bar{u})^T\}^{-1} \qquad (2)$$

with the expectation operation $E\{\cdot\}$, $\bar{c} = E\{c\}$, and $\bar{u} = E\{u\}$. We conducted experiments on simulated data. For the creation of a dataset, the MNIST dataset [7] was used as particle distribution. It contains 70000 digital images of handwritten

numbers between the digits zero and nine, where each image has a size of 28×28 pixels. The simulation of the voltage signal was based on the Langevin model of paramagnetism. The field of view (FOV) was defined to have size $20.4 \times 20.4\ \mathrm{mm}^2$, the frequency ratio for the Lissajous trajectory was $f_x/f_y = 31/32$, the particle size was 30 nm, and the body temperature of humans was assumed inside the simulation. To prevent inverse crime, the images were upscaled to 40×40 pixels. The voltage signals were corrupted with white Gaussian noise at a signal-to-noise ratio (SNR) of 20 dB. To cover the whole FOV, the dataset was augmented by three random rigid motions for each digit. In total, the dataset had 4×70000 voltage signals. All images showing a five form the test dataset (25252 samples) and the images of the other 9 digits were used for training the NNs.

III. Results

The approaches were compared with three error measures: MSE, MAE, and structural similarity (SSIM) index. For all measures, the average and standard deviation ($\pm$) over the whole test dataset were calculated (see Tab. 1). Both NNs outperform the linear MMSE estimator. The NN trained with MAE loss turned out to be superior to the one optimized under MSE loss with respect to the SSIM. Therefore, in Fig. 2, a few test images reconstructed by the NN with MAE loss are shown exemplarily. Even though the letter five was not included in the training data, it is quite accurately reconstructed. We used the trained model also for the reconstruction of vessel-like structures from their voltage signals (SNR of 20 dB). Examples can be found in Fig. 3. The reconstruction of this structures is reasonable but not as good as for the fives of the MNIST database (see Fig. 2).

IV. Discussion

The experiments verifies that for the reconstruction in MPI, nonlinear approaches that go beyond demanding $\hat{c} \geq 0$ are favorable. Furthermore, the nonlinear networks appear as a promising method for learning the inverse system. The results indicate that there is a significant difference between the structures of the vessel-like phantom and the MNIST numbers. It seems promising to present all different kinds of structures in the training dataset. However, the coarse structures as well as the background are reconstructed well. This shows the generalization ability of the network and indicates that the trained NN learned to invert the physical model. One drawback of the approach is the required amount of training data. In future research, we will focus on strategies to tackle the problem and apply the proposed technique to real data.

V. Conclusions

We proposed an end-to-end trained neural network capable of reconstructing MPI images from the voltage signal. The network can reconstruct structures that have never been presented during training. Since the networks outperform the linear MMSE estimator quite significantly, it becomes obvious that our nonlinear approach can learn and exploit the statistics of the data much better than a linear method.

Table 1: *Results for the networks and the MMSE estimator on the MNIST test data containing only the digit five.*

	MSE	MAE	SSIM index
NN (MSE loss)	0.0041 $\pm$ 0.0024	0.0232 $\pm$ 0.0086	0.9214 $\pm$ 0.0261
NN (MAE loss)	0.0042 $\pm$ 0.0024	0.0209 $\pm$ 0.0075	0.9510 $\pm$ 0.0246
Linear MMSE estimator	0.0087 $\pm$ 0.0038	0.0490 $\pm$ 0.0122	0.4803 $\pm$ 0.0895

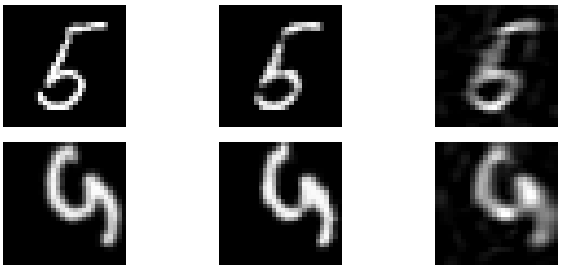

Figure 2: *Reconstructed MNIST images. First column: ground truth. Second column: reconstructions of NN trained with MAE loss. Third column: MMSE reconstructions.*

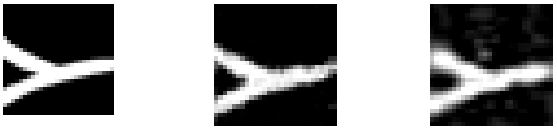

Figure 3: *Vessel images. From left to right; Ground truth, reconstruction of NN trained with MSE (MSE: 0.0110, MAE: 0.0411, SSIM index: 0.9081), and MMSE reconstruction (MSE: 0.0134, MAE: 0.0686, SSIM index: 0.5083).*

AUTHOR'S STATEMENT

This work was supported by the German Research Foundation under grant number ME 1170/7-1. Authors state no conflict of interest.

REFERENCES

[1] T. Knopp, J. Rahmer, T. F. Sattel, S. Biederer, J. Weizenecker, B. Gleich, J. Borgert, and T. M. Buzug. Weighted Iterative Reconstruction for Magnetic Particle Imaging. *Phys. Med. Biol.*, 55(6):1577-1589, 2010. doi: 10.1088/0031-9155/55/6/003.

[2] T. Hatsuda, T. Takagi, A. Matsuhisa, M. Arayama, H. Tsuchiya, S. Takahashi, and Y. Ishihara. Basic Study of Image Reconstruction Method using Neural Networks with Additional Learning of Magnetic Particle Imaging. *Int. J. Magn. Part. Imaging*, 2(2), 2016. doi: 10.18416/ijmpi.2016.1611002.

[3] B. G. Chae. Neural Network Image Reconstruction for Magnetic Particle Imaging. *ETRI J.*, 39(6):841-850, 2017. doi: 10.4218/etrij.2017-0094.

[4] E. Kang, J. Min, and J. C. Ye. A deep convolutional neural network using directional wavelets for low-dose X-ray CT reconstruction. *Med. Phys.*, 44(10):e360-e375, 2017. doi: 10.1002/mp.12344.

[5] K. H. Jin, M. T. McCann, E. Froustey, and M. Unser. Deep Convolutional Neural Network for Inverse Problems in Imaging. *IEEE Trans. Image Process.*, 26(9):4509-4522, 2017. doi: 10.1109/TIP.2017.2713099.

[6] B. Zhu, J. Z. Liu, S. F. Cauley, B. R. Rosen, and M. S. Rosen. Image reconstruction by domain-transform manifold learning. *Nature*, 555(7697):487-492. doi: 10.1038/nature25988.

[7] Y. LeCun, L. Bottou, Y. Bengio, and P. Haffner. Gradient-Based Learning Applied to Document Recognition. *Proc. IEEE*, 86(11):2278-2324, 1998. doi: 10.1109/5.726791.

[8] J. M. Mendel. *Lessons in Estimation Theory for Signal Processing, Communications, and Control*. Prentice Hall, 1995.